Hindawi
Mathematical Problems in Engineering
Volume 2022, Article ID 6901534, 15 pages
https://doi.org/10.1155/2022/6901534

Research Article

Study on Leakage Model of Typical Penetration of Closed Structures Based on Porous Media Seepage Theory

Xin Lin[1] **and Zhehua Du**[2]

[1]*Hubei Province Engineering Consulting Co., LTD., Wuhan, Hubei, 430071, China*
[2]*Wuhan Second Ship Design and Research Institute, Wuhan, Hubei, 430205, China*

Correspondence should be addressed to Xin Lin; 754726516@qq.com

Received 23 November 2021; Accepted 28 January 2022; Published 28 February 2022

Academic Editor: Muhammad Afzal Rana

Quantitative prediction of penetration leakage rate has not been reported so far. The theoretical prediction method of leakage rate of typical penetration static seal structure of closed structure is studied. Based on porous media seepage mechanics, the relationship between leakage rate and microstructure parameters is established, and a new prediction model of the leakage rate of sealing structures is proposed. Then, the relationship between seal-specific pressure and microstructure parameters is obtained by the Hertz contact mechanics model. Finally, the leakage rate calculation, which is independent of any experimental data, is obtained innovatively. The new model is used to predict the leakage rate of penetration, and the theoretical prediction results are compared with the experimental measurement results. It is proved that the two agree well, which verifies the effectiveness of the model. The prediction model based on this method can well reflect the effects of rough surface morphology, material mechanical properties, sealing load, high temperature, and high pressure on the leakage rate. The leakage rate prediction model proposed in this paper is independent of the experimental regression coefficient and can realize the conversion relationship between different sealing media, sealing materials, and working conditions.

1. Introduction

Nuclear power plant containment is a typical closed structure. The pressure boundary formed by the containment and much perforated equipment, components, and pipelines penetrating the containment is not only the last barrier between the internal equipment or system and the environment but also a very important barrier related to safety. Penetration is usually the main way of containment leakage in nuclear power plants. Penetration refers to the gaping hole equipment, components, pipelines, and isolation valves penetrating the closed structure. There are a large number of penetrations. Ensuring their sealing integrity under various working conditions is an important content in the design of closed structures [1–3]. Penetration can be divided into electrical penetration and mechanical penetration. The principal function of the electrical penetration assembly is to connect the electrical equipment to the outside of the containment to control the equipment inside the containment. There are two types of mechanical penetration: one is fuel transportation penetration; the other is mechanical pipe penetration.

In order to find an effective method to improve the reliability of penetration seal, researchers at home and abroad have carried out a lot of research. Argonne National Laboratory, Sandia National Laboratory, and Idaho nuclear engineering laboratory have conducted extensive research on the reliability of penetration seal structure of 22 nuclear power plants [4, 5], put forward some common problems in penetration seal, and discussed the influence of high temperature and high pressure on gasket sealing performance from the perspective of flange warpage and deformation. Based on experimental research, some researchers qualitatively discussed the damage of mechanical properties of sealing materials caused by high temperature and irradiation [4–7]. In addition, many scholars have used three-

dimensional finite element technology to study the mechanical deformation of penetration system under serious accidents [8, 9]. In addition, many scholars have established a series of models and theories using porous media seepage theory. However, there are few reports on the quantitative prediction of the leakage rate of penetration seal structure.

Quantitative analysis of the leakage rate is the basis of the safety design of penetration seal structure. However, the quantitative prediction research on the leakage rate of penetration seal structure has not been reported so far. The main reason is that people's understanding of the leakage mechanism of seal structure is not clear enough. Only by deeply studying the microleakage mechanism of sealing structure can the quantitative relationship between leakage rate and various influencing factors be established, and the research on penetration sealing characteristics can be developed from "qualitative" to "quantitative." Existing leakage rate calculation models are semiempirical without exception; that is, there are regression coefficients in the model that has unclear physical meaning and need to be fitted with experimental results. The dependence on experimental research makes these calculation models unable to be applied to the prediction of gasket leakage rate of nonstandard structure, special working conditions, and special gas without experimental data. The key problem is that there is no appropriate leakage mechanism model of penetration seal structure.

The purpose of this paper is to introduce the porous media seepage theory and build the sealing microleakage mechanism model based on the essence of gas leakage phenomenon. The focus is to establish the quantitative relationship between microfine structure and macromeasure and then put forward a prediction and calculation method of leakage rate independent of experimental regression parameters. On this basis, the accuracy of the prediction model is verified by experiments. This method can effectively analyze the coupling effect of interface microstructure and material macromechanical properties on the leakage rate. It provides a theoretical basis for the development and design of penetration seal structure and provides guarantee for environmental quality and safety.

2. Leakage Mechanism Model of the Static Seal Interface

The interface leakage of static seal generally refers to the leakage of fluid through the rough contact surface between the flange and sealing material. The workpiece surface is always rough in varying degrees. The contact surface between the flange and the sealing material is not particularly close, and the sealing medium can leak out from these gaps. The close contact between the two sealing surfaces is realized by applying a compressive load, to reduce the pore space in the sealing gap and increase the flow resistance. Under the action of internal and external pressure differences, the medium will leak from a high-pressure environment to a low-pressure environment. According to different flow paths, leakage can be structured in interface leakage (seepage through different contact material surfaces) and seepage leakage (seepage from the inside of sealing material). The density of materials used for sealing is generally bulky, and the proportion of seepage leakage is very small. Therefore, this paper is only focused on the study of interface leakage.

The gas flow characteristics in a rough gap are studied using the mesoscopic lattice Boltzmann method (LBM). First, the virtual interface leakage channel is established based on the three-dimensional numerical reconstruction technology of rough surface, and then, the influence of gas rough interface on gas flow is analyzed by LBM simulation. Figures 1 and 2 show the rough numerical surface constructed based on Gauss distribution and the LBM model used.

The simulation results show that when the channel height remains unchanged, the fluid flow in the interface still retains the characteristics of plane Poiseuille flow. Therefore, a rough flow factor can be defined Φ_σ:

$$\Phi_\sigma = \frac{Q_0}{Q_p}. \tag{1}$$

In the formula, Q_0 represents the volume flow rate of the rough surface channel, and Q_p represents the volume flow rate of the smooth plate channel with the same gap height. According to the model of parallel plate flow,

$$Q_p = \frac{Bh^3}{12\mu L} \times (p_2 - p_1). \tag{2}$$

In the formula, h represents the clearance height of the smooth flat plate channel, B is the flow channel width, l is the flow channel length, p_2 is the internal pressure, and p_1 is the external ambient pressure. Φ_σ is only related to the characteristics of rough surface, which can be defined as dimensionless roughness σ^* function of ($\sigma^* = \sigma/T$), where s and T is two statistical parameters of a rough surface, namely, roughness(μm) and autocorrelation scale(μm). According to the numerical results $\Phi\sigma - \sigma^*$, the curve is shown in Figure 3 (1), and its function expression is

$$\Phi_\sigma = \exp(-0.9242\sigma^* + 0.7026). \tag{3}$$

Based on the numerical results, the height flow factor is further defined Φ_h to characterize the effect of gap height change on gap flow at the rough interface, and its expression is

$$\Phi_h = \frac{Q}{Q_0}. \tag{4}$$

In the formula, Q_0 is the initial clearance height h_0 obtained in (2). Q represents the volume flow corresponding to the actual height h. When the characteristics of a rough surface are certain, Φ_h is only the dimensionless gap height h^* ($h^* = h/\sigma$). Figure 3 (2) shows the curve fitted according to the numerical calculation results, and its functional relationship is

$$\Phi_h = \exp(0.7545h^* - 3.673). \tag{5}$$

In this way, when the characteristic parameters of a rough surface and the change of interface gap height are

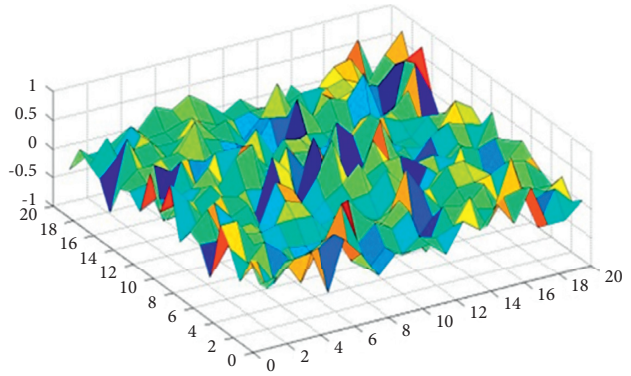

Figure 1: Numerical random surface satisfying Gauss distribution.

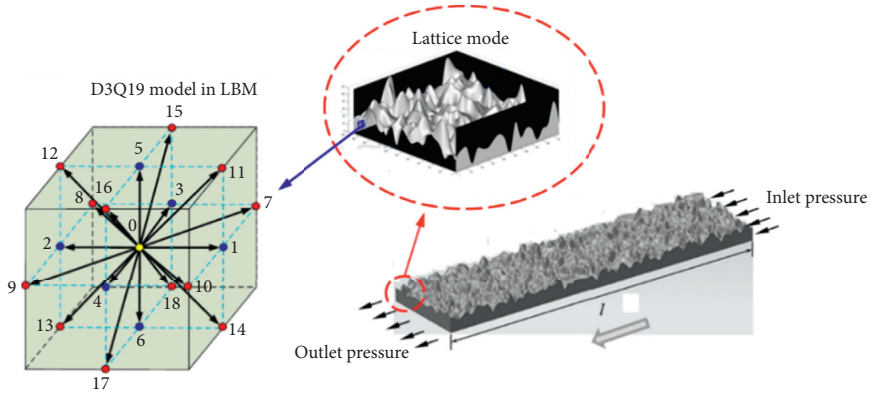

Figure 2: Schematic diagram of LBM model of interface microporous structure leakage.

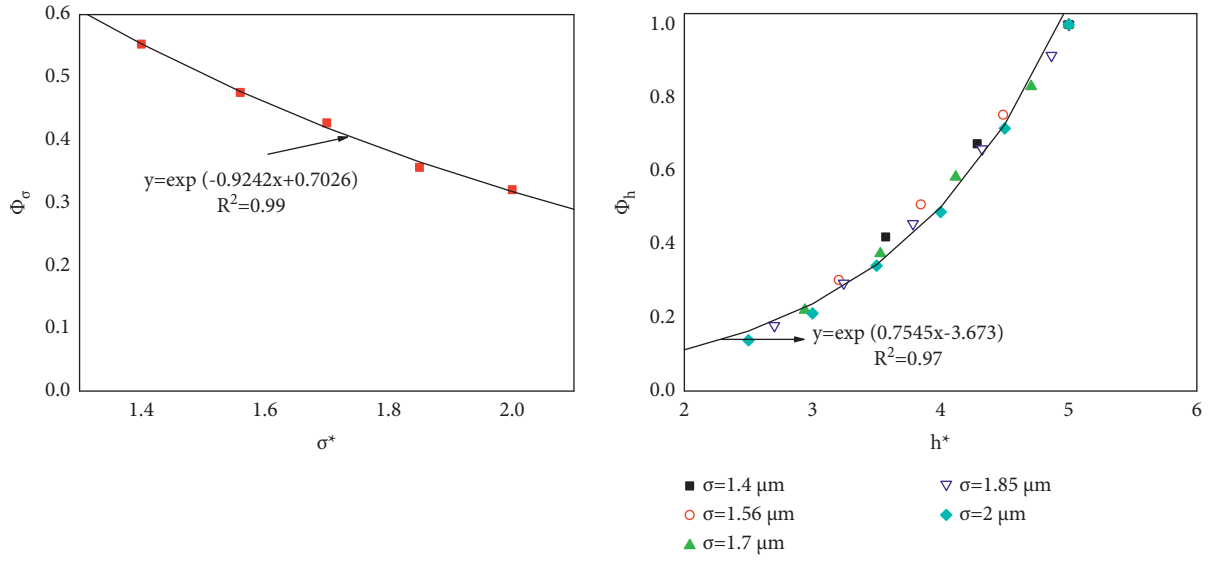

Figure 3: Calculation results and fitting curves of two flow factors. (a) Roughness factor φ_σ fitting. (b) Height factor fitting.

known, the gas volume flow through the interface microporous structure can be calculated using the following formula:

$$Q = \Phi_\sigma \cdot \Phi_h \cdot Q_p. \tag{6}$$

Formula (6) effectively reveals the flow characteristics of gas in the sealing interface, and it offers an effective way to build the interface leakage mechanism model based on the numerical calculation method.

3. Construction Method of a Theoretical Model of the Penetration Leakage Rate of Typical Structures

Taking the manhole pressure cover as an example, the penetration leakage theoretical model of typical structures is constructed [4–7].

3.1. Finite Element Analysis Model. The pressure cover of the manhole is one of the main penetrations installed on the closure. Structurally, it can classify as a large-diameter nonstandard bolt flange gasket structure. The sealing principle is to use the pretightening force of the bolt to make the cover compress the gasket and from contact pressure on the sealing surface through the elastic deformation of the gasket, to achieve the sealing effect. Figure 4 is the assembly diagram of the pressure cover of the manhole and the established three-dimensional schematic diagram [8].

Because of the characteristics of nonstandard and large diameter, some theoretical analysis methods only apply to standard bolt flange gasket and cannot be directly applied to the analyses of mechanical deformation characteristics of pressure cover, and the finite element analysis method is still necessary. To control the leakage rate of the static seal structure of the manhole, it is necessary to clarify the main influencing factors and the variation law of the leakage rate for these factors. Therefore, it is the key to constructing the theoretical prediction model of the leakage rate of the pressure cover of the manhole [8, 9].

The method of constructing the theoretical model of pressure covers leakage rate is divided into three steps. First, according to the microcosmic mechanical analysis of the rough element of sealing contact surface, the microcosmic leakage mechanism model is constructed. Second, the influence of various factors on the contact seal of sealing surface is analyzed according to the macrofinite element method. Third, using the coupling relationship between sealing surface contact seal and the microcosmic leakage mechanism, the leakage rate prediction model of pressure cover sealing structure is established. This method realizes the effective coupling of microdetailed structural analysis and macromechanical characteristic analysis and does not include any experimental regression coefficient. It can effectively analyze the change law and influencing factors of pressure cover leakage rate, and it is not difficult to control its leakage rate [5, 10–12].

The cover plate is in the form of flat plate reinforcement, and it is not rotational axisymmetry. Therefore, the 1/4

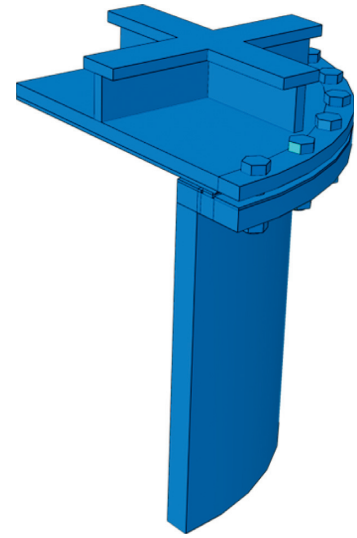

Figure 4: 3D schematic diagram of pressure cover of the manhole.

model is utilized to simplify the analyses. The physical parameters used in the calculation are as follows. The elastic modulus of the cover plate, lower flange, and cylinder is 210000 MPa and Poisson's ratio is 0.3. The elastic modulus of bolts and nuts is set to 203000 MPa, and Poisson's ratio is 0.3; The gasket is made of neoprene with a thickness of 5 mm, and its stress-strain curve is obtained by consulting the literature (refer to Figure 5) [13, 14].

The flange joint has axisymmetric properties in structure, load, and constraint. Therefore, boundary symmetry constraints are imposed on the two symmetry planes of the whole finite element model to constrain the circumferential displacement of the two plane nodes. At the same time, to limit the overall rigid body displacement of the joint, fixed boundary conditions are imposed on the truncated surface of the cylinder.

Calculate the bolt design load of flange joint during assembly and operation, with gasket pretension ratio pressure Y and gasket factors M.

(1) Determine the minimum bolt load required under operating conditions W_{m1}

$$W_{m1} = \frac{\pi}{4} D_G^2 p + 2b\pi D_G m p, \tag{7}$$

where D_G is the iameter at the center circle of the gasket compression stress, mm, b is the effective sealing width of gasket, mm, p is the pressure of medium in the vessel, MPa, and m is the gasket coefficient.

(2) Determine the minimum bolt load required for the pretension gasket W_{m2}

$$W_{m2} = \pi b D_G y, \tag{8}$$

where y is the gasket pretension ratio pressure, MPa.

The design load of the bolt can be obtained by bringing in the gasket parameters:

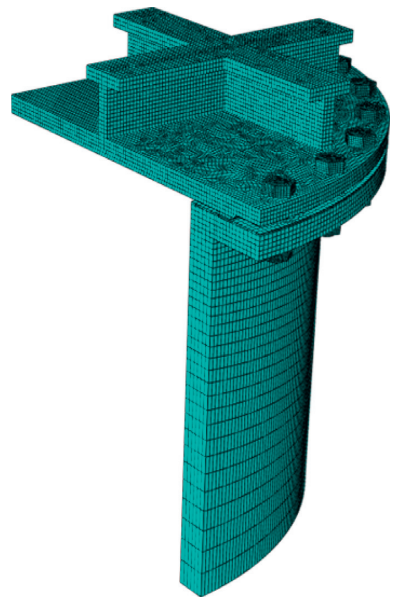

Figure 5: Finite element model of plane sealing structure.

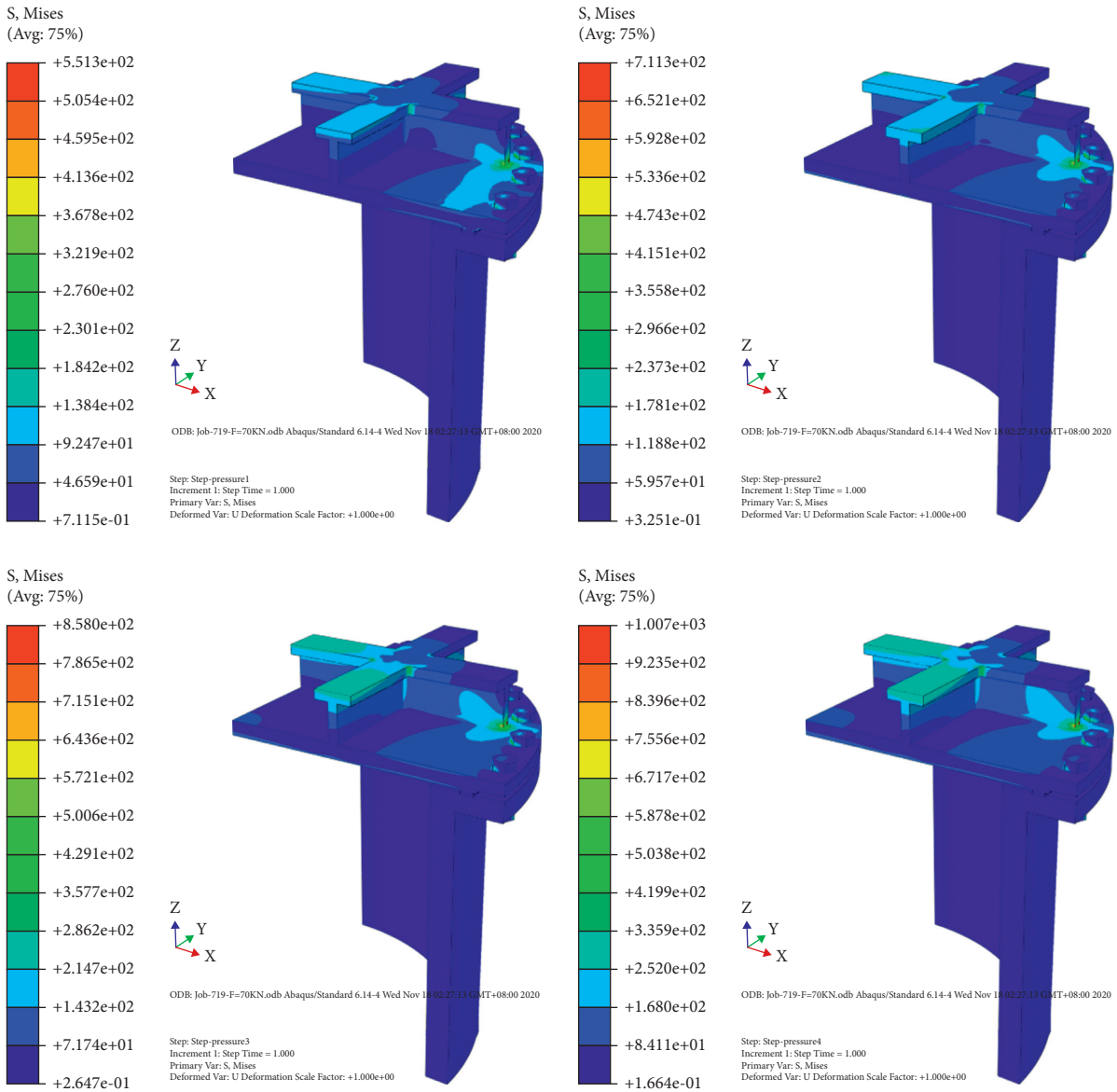

Figure 6: Stress distribution of structure under different pressures. (a) $F = 70$ kN $\triangle P = 0.45$ MPa. (b) $F = 70$ kN $\triangle P = 1$ MPa. (c) $F = 70$ kN $\triangle P = 1.5$ MPa. (d) $F = 70$ kN $\triangle P = 2$ MPa.

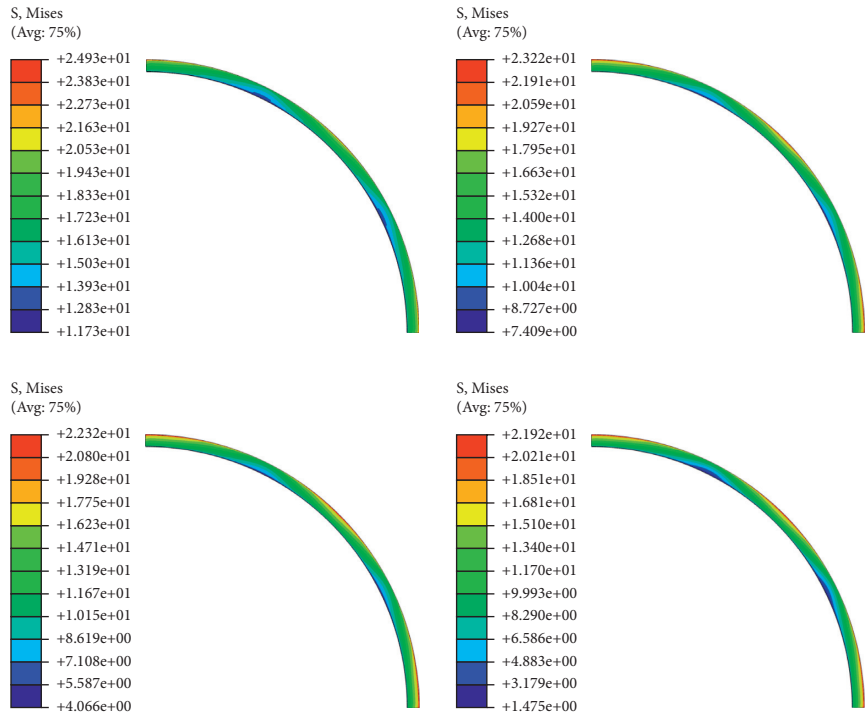

Figure 7: Stress distribution of gasket under different pressures. (a) $F = 70$ kN $\Delta P = 0.45$ MPa. (b) $F = 70$ kN $\Delta P = 0.45$ MPa. (c) $F = 70$ kN $\Delta P = 1.5$ MPa. (d) $F = 70$ kN $\Delta P = 2$ MPa.

$$W_B = \mathrm{Max}(W_{m1}, W_{m2}). \tag{9}$$

The design load of a single bolt can be obtained by bringing in the gasket parameters:

$$F = \frac{W_B}{28} \approx 70kN. \tag{10}$$

The calculation process is roughly as follows. To make the analysis easier to converge, a tiny bolt force is applied in the first analysis step to establish the contact relationship between various surfaces smoothly. In the second analysis step, the bolt force is brought to the pretension. In the third analysis step, the pressure under various working conditions is applied to the flange and the inner wall of the cover [15, 16].

3.2. Finite Element Analysis Results. The gasket material is neoprene. Considering the stress distribution and the leakage rate of the gasket when the bolt pretension f is 70 kN, 80 kN, 90 kN, 100 kN, and 110 kN, the medium working pressure is, respectively, $\Delta P = 0.45$ MPa, 1 MPa, 1.5 MPa, and 2 MPa. When the pretension is 70 kN and considering the change of working pressure, the overall stress distribution and gasket stress distribution are shown in Figure 6 respectively. When the medium working pressure is 0.45 MPa and considering the change of pretension, the overall stress distribution and gasket stress distribution are shown in Figures 8 and 9, respectively [17].

It can be perceived from Figures 6 and 7 that, under the same pretension, the stress distribution of the overall structure of the bolt flange is similar, the stress is concentrated at the connection between the bolt and nut and the connection between the stiffener and the cover, and the maximum stress value increases significantly with the increase of pressure, while the gasket stress value decreases with the increase of pressure. According to Figures 8 and 9, under the same medium pressure, with the increase of pretension, the overall maximum stress value increases, and the gasket stress value also increases. Considering that large-diameter flange is prone to warpage under large internal pressure, the following figure and table list the stress value of the specific structure and the change of flange angle under pressure change and pretension change, respectively.

It can be seen from Tables 1 and 2 that, under the given pretension and pressure, the flange angle is less than 0.3° specified by ASME. With the increase of pressure and pretension, the flange angle increases. Considering the maximum stress strength, it can be seen from Figure 10 that when the medium pressure is not high (e.g., $\triangle P = 0.45$ MPa), the stress of the cover plate is less than the maximum value of the material given in the project, and when the pressure increases, the maximum stress may exceed the material yield strength (e.g., $\triangle P = 2.0$ MPa). The maximum stress in the whole seal occurs at the welding between the stiffener and the cover, and the maximum stress in the bolt is also large. It is necessary to consider whether the bolt strength meets the requirements [13–15].

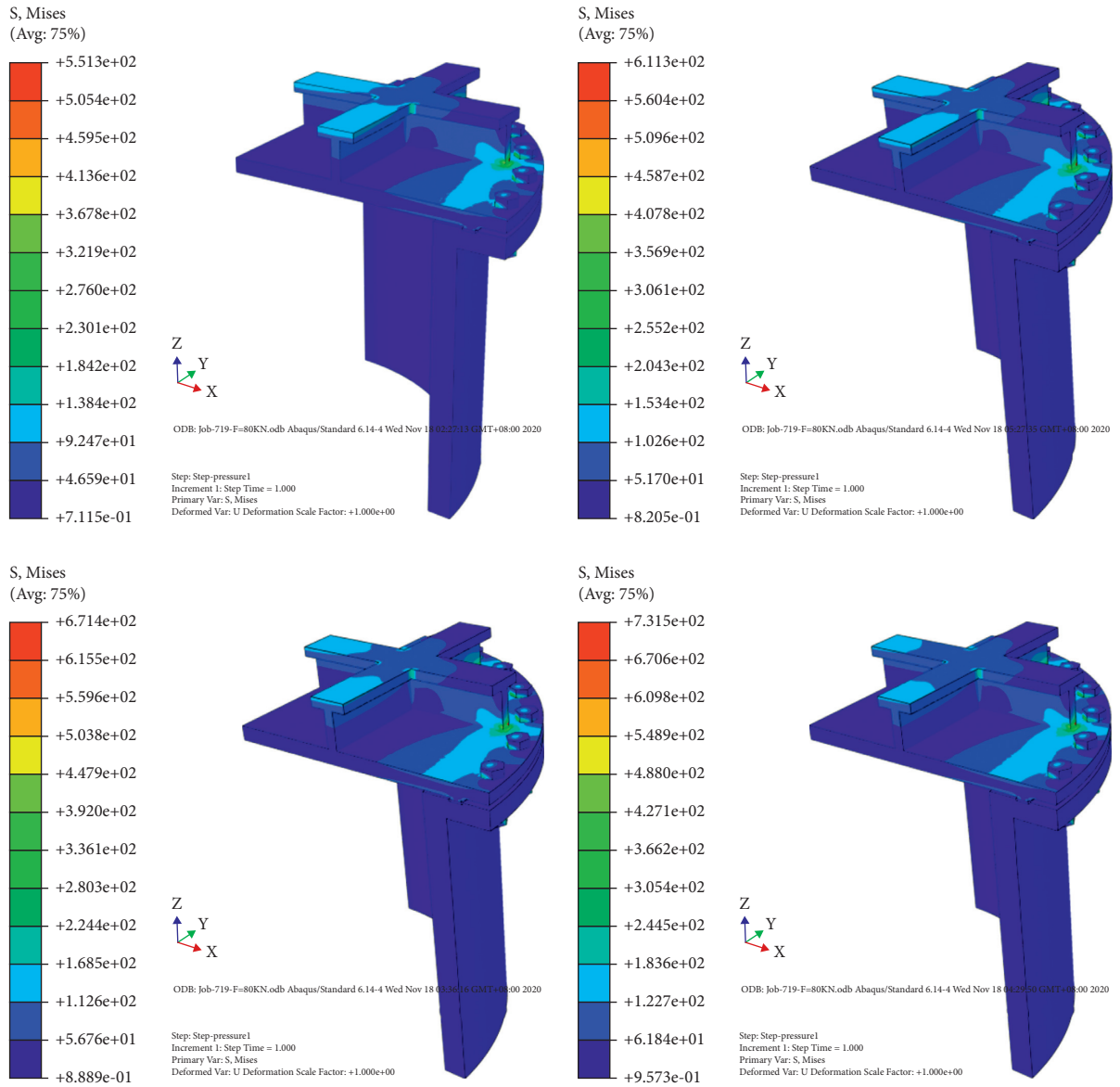

FIGURE 8: Overall stress distribution of structure under different pretensions. (a) $F = 70$ kN $\Delta P = 0.45$ MPa. (b) $F = 80$ kN $\Delta P = 0.45$ MPa. (c) $F = 90$ kN $\Delta P = 0.45$ MPa. (d) $F = 100$ kN $\Delta P = 0.45$ MPa.

As the sealing performance is related to the stress at the contact surface, Figure 11 shows a schematic diagram of the stress distribution on the gasket contact surface varying with pressure under four pretensions. It can be seen from the figure that, under the following conditions, all actual sealing width is gasket width, and the contact stress of gaskets increases with the increase of radial distance. When the pretension is constant, the contact stresses decreases with the increase of medium pressure. When the pressure is constant, the contact stress increases with the increase of pretension. For further comparison, Figure 12 is a schematic diagram of the variation of the average contact stress with pressure at different pretensions. It can be seen that the average contact stress decreases linearly with the medium pressure. The greater the pretension, the greater the average contact stresses under the same pressure. Under different preloads, when the medium pressure increases from 0.45 MPa to 2.0 MPa, the average contact stress decreases by about 26%.

3.3. Fitting Formula of Leakage Rate. The calculation data and details fitted by the leakage rate formula of the pressure cover of the manhole are shown in Table 3.

3.4. Quantitative Prediction of Leakage Rate. The previous section mainly discussed the stress distribution of the entire sealing structure and each component under different medium pressures and pretensions. This section analyzes it from the perspective of the leakage rate. Under certain other conditions, the contact stress increases with the increase of

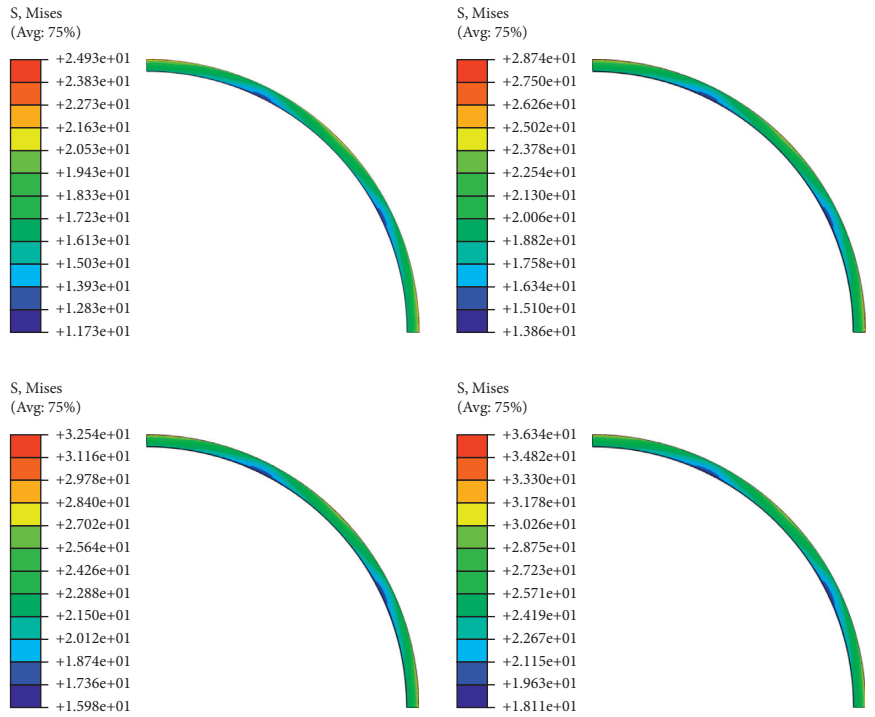

Figure 9: Stress distribution of gasket under different pretensions. (a) $F = 70$ kN $\Delta P = 0.45$ MPa. (b) $F = 80$ kN $\Delta P = 0.45$ MPa. (c) $F = 90$ kN $\Delta P = 0.45$ MPa. (d) $F = 100$ kN $\Delta P = 0.45$ MPa.

Table 1: Stress value and flange angle of each component under different pressures ($F = 70$ kN).

Medium pressure (MPa)	Maximum gasket stress (MPa)	Maximum cover plate stress (MPa)	Maximum stress value of cover plate (MPa)	Flange angle/°
0.45	24.93	471.0	551.3	0.084647
1	23.22	609.9	711.3	0.142271
1.5	22.32	737.9	858.0	0.196896
2	21.92	866.7	1007	0.251075

Table 2: Stress value and flange angle of each component under different pretensions ($\Delta P = 0.45$ MPa).

Pretension (kN)	Maximum gasket stress (MPa)	Maximum cover plate stress (MPa)	Maximum stress value of cover plate (MPa)	Flange angle/°
70	24.93	471.0	551.3	0.084647
80	28.74	523.6	611.3	0.089858
90	32.54	579.0	671.4	0.095071
100	36.34	637.2	731.5	0.100287

bolt pretension, but the structural stress increases at the same time. Therefore, the material damage and failure caused by excessive pretension should be avoided. According to the theoretical analysis of leakage rate, the actual roughness is Ra3.2 [18, 19]. Under different pretensions, the intermediate parameters and final leakage rate are calculated, respectively, as shown in Tables 4–7.

Figure 13 is a comparison diagram of gasket leakage rate under two different pretensions. It can be seen that, regardless of the pretension, the gasket leakage rate increases with the increase of medium pressure, and the gap of leakage rate between different pretensions increases with the increase of pressure [20–22].

4. Leakage Prediction and Test Verification of Typical Penetration

The leakage rate prediction method of complex sealing structure of containment penetration is shown in Figure 13. In addition to the theoretical prediction of typical penetration, the accuracy of the prediction model is verified by experiments. There are five types of typical penetration tested, including a pressure gate, lifting hole, isolation valve, butterfly valve, and ball valve.

Figures 14 and 15 display the device diagram and schematic diagram of the leakage rate test system of the pressure valve. The diameter of circular gate is 800 mm, with

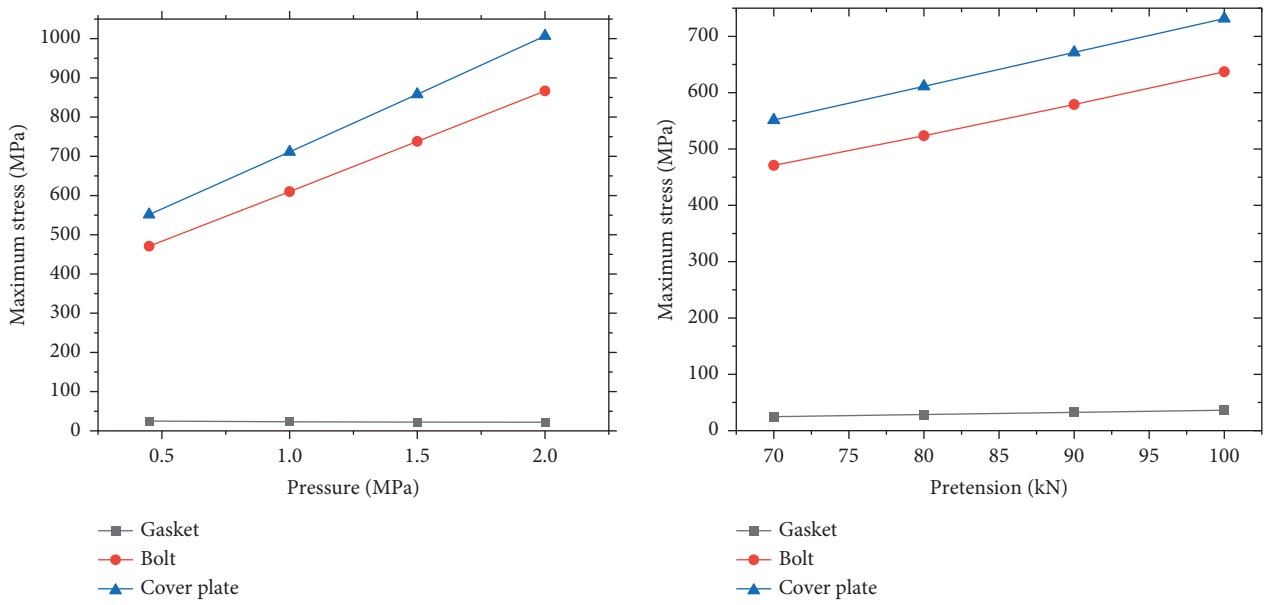

Figure 10: Variation of maximum stress of each component with pressure and pretension. (a) Different pressures. (b) Different pretensions.

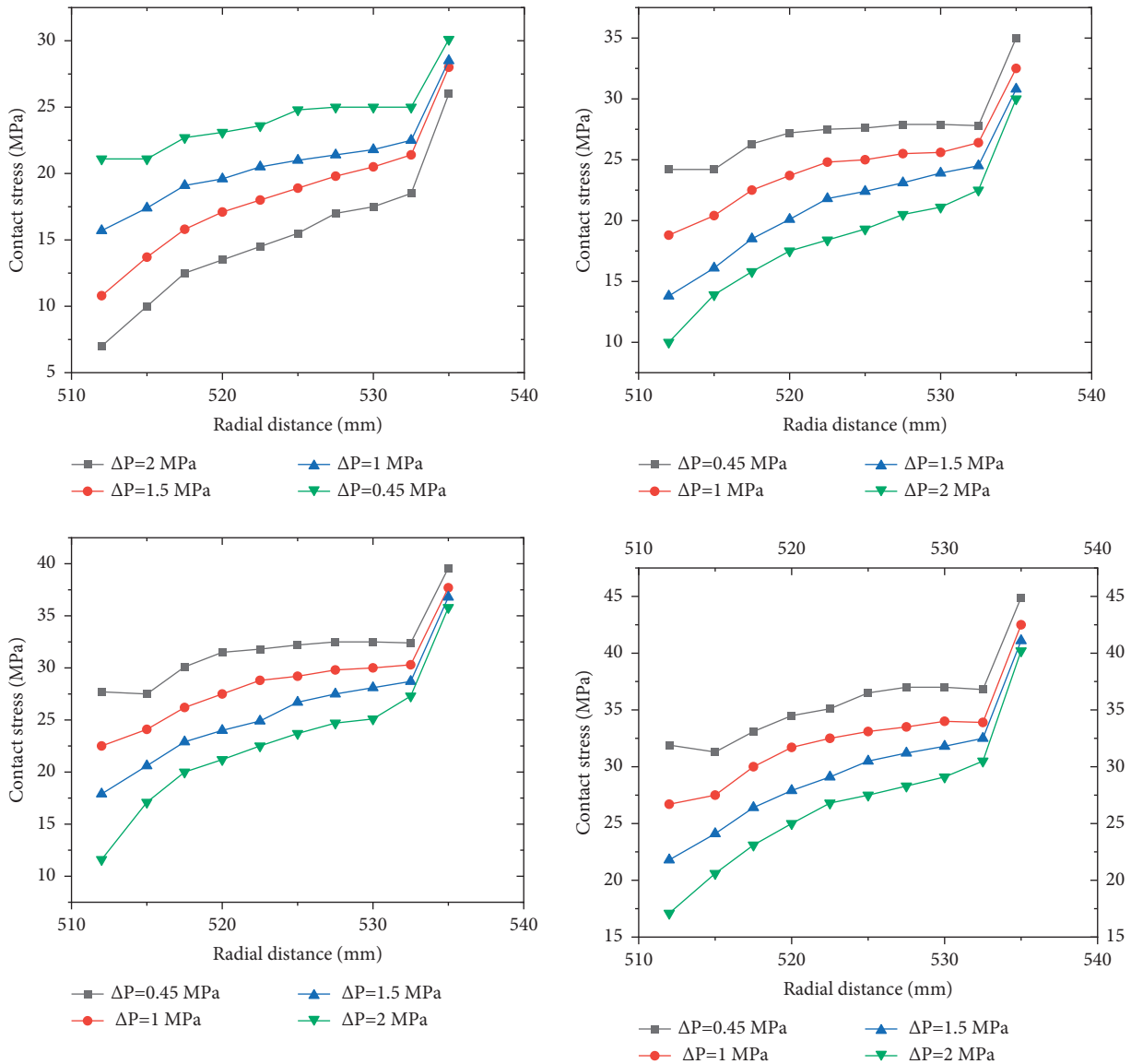

Figure 11: Variation of gasket contact stress distribution with pressure under different pretensions. (a) $F = 70$ kN. (b) $F = 80$ kN. (c) $F = 90$ kN. (d) $F = 100$ kN.

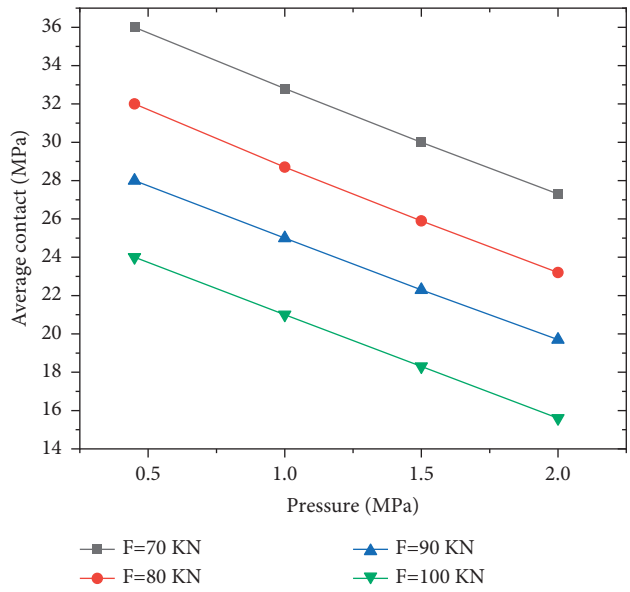

Figure 12: Variation of average contact stress.

Table 3: Fitting of calculation formula for leakage rate of manhole pressure cover.

Initial sealing conditions F/kN		100			
Circumference of seal ring, B/m		3.216			
Surface composite roughness, σ/m		3.2×10^{-6}			
Rubber material hardness, HA		60			
Kinematic viscosity of medium, μ/(Pa.s)	Pressure P/MPa	0.45	1	1.5	2
	Dry air	1.80×10^{-5}	1.80×10^{-5}	1.80×10^{-5}	1.80×10^{-5}
	Saturated steam	8.00×10^{-5}	5.90×10^{-5}	5.30×10^{-5}	4.69×10^{-5}
Contact width, L/m		0.023			
Permeability, K	Rough flow factor, Φ_σ	$\Phi_\sigma = \exp(-0.9242\sigma^* + 0.7026)$.			
	Height flow factor, Φ_h	$\Phi_h = \exp(0.7545h^* - 3.673)$.			
	Dimensionless gap height, h^*	$h^* = -1.056S_G^{*0.5806} + 1.023$.			
	Dimensionless mean contact stress, S_G^*	$S_G^* = -0.04679\Delta P + 0.3179$.			
	Permeability, K	$K = \Phi_\sigma\Phi_h(h^*)^3(h^0)^2/12$.			
The formula of leakage rate		$Q_v = KBh_0/\mu L(p_1^2 - p_2^2/2p_1)$.			

Table 4: Calculation process quantity of gasket leakage rate ($F = 70$ kN).

Medium pressure (MPa)	Dimensionless sealing stress, S_G^*	Leakage channel height, h (μm)	Height factor	Roughness factor	Leakage, Q/(m^3/s)
0 €.45	0.201497	3.88094419	0.062725	0.1048906	1.17973–7
1	0.175697	4.0848284	0.065776	0.1048906	3.20555–7
1.5	0.152423	4.27982389	0.068833	0.1048906	5.78731–7
2	0.129104	4.48820256	0.072256	0.1048906	9.34191–7

Table 5: Calculation process quantity of gasket leakage rate ($F = 80$ kN).

Medium pressure/ MPa	Dimensionless sealing stress, S_G^*	Leakage channel height, h/μm	Height factor	Roughness factor	Leakage, Q/(m^3/s)
0 (E).45	0.233311	3.64406723	0.059358	0.1048906	9.24197–8
1	0.207489	3.83518906	0.06206	0.1048906	2.50315–7
1.5	0.184153	4.01669524	0.064741	0.1048906	4.49974–7
2	0.160958	4.20695282	0.067674	0.1048906	7.20558–7

Table 6: Calculation process quantity of gasket leakage rate ($F = 90$ kN).

Medium pressure (MPa)	Dimensionless sealing stress, S_G^*	Leakage channel height, h (μm)	Height factor	Roughness factor	Leakage, Q/(m^3/s)
0.45	0.265123	3.42042249	0.056345	0.1048906	$7.25471E-8$
1	0.239291	3.60109403	0.058767	0.1048906	$1.96223E-7$
1.5	0.215903	3.77187469	0.061152	0.1048906	$3.51954E-7$
2	0.192712	3.94906639	0.063729	0.1048906	$5.61256E-7$

Table 7: Calculation process quantity of gasket leakage rate ($F = 100$ kN).

Medium pressure (MPa)	Dimensionless sealing stress, S_G^*	Leakage channel height, h (μm)	Height factor	Roughness factor	Leakage, Q/(m^3/s)
0.45	0.296932	3.20780136	0.053622	0.1048906	$5.695E-8$
1	0.27109	3.37975131	0.055814	0.1048906	$1.54066E-7$
1.5	0.24768	3.54155993	0.057958	0.1048906	$2.7612E-7$
2	0.224423	3.70880364	0.06026	0.1048906	$4.39616E-7$

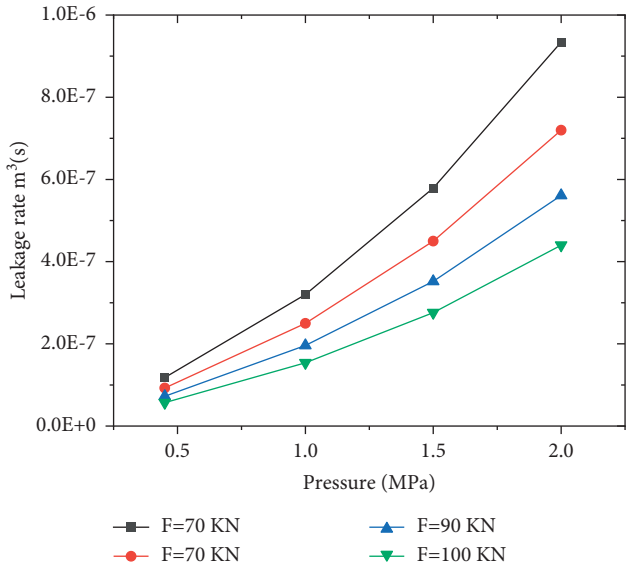

Figure 13: Change of gasket leakage rate and pressure under different pretensions.

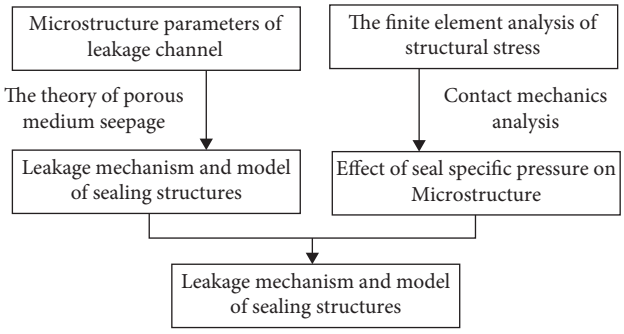

Figure 14: Construction method of typical penetration prediction model.

concave face outward and convex face inward. The inside of the gate is connected to a fully welded sealed sealing chamber, and the test gas is supplied to the sealing chamber through the air inlet hole. The flow supplement method is adopted in the test, and its schematic diagram is given in Figures 1–3. The gas cylinder fills the test space, and the test pressure is automatically maintained constant through the pressure regulator. The measured supplementary flow is the

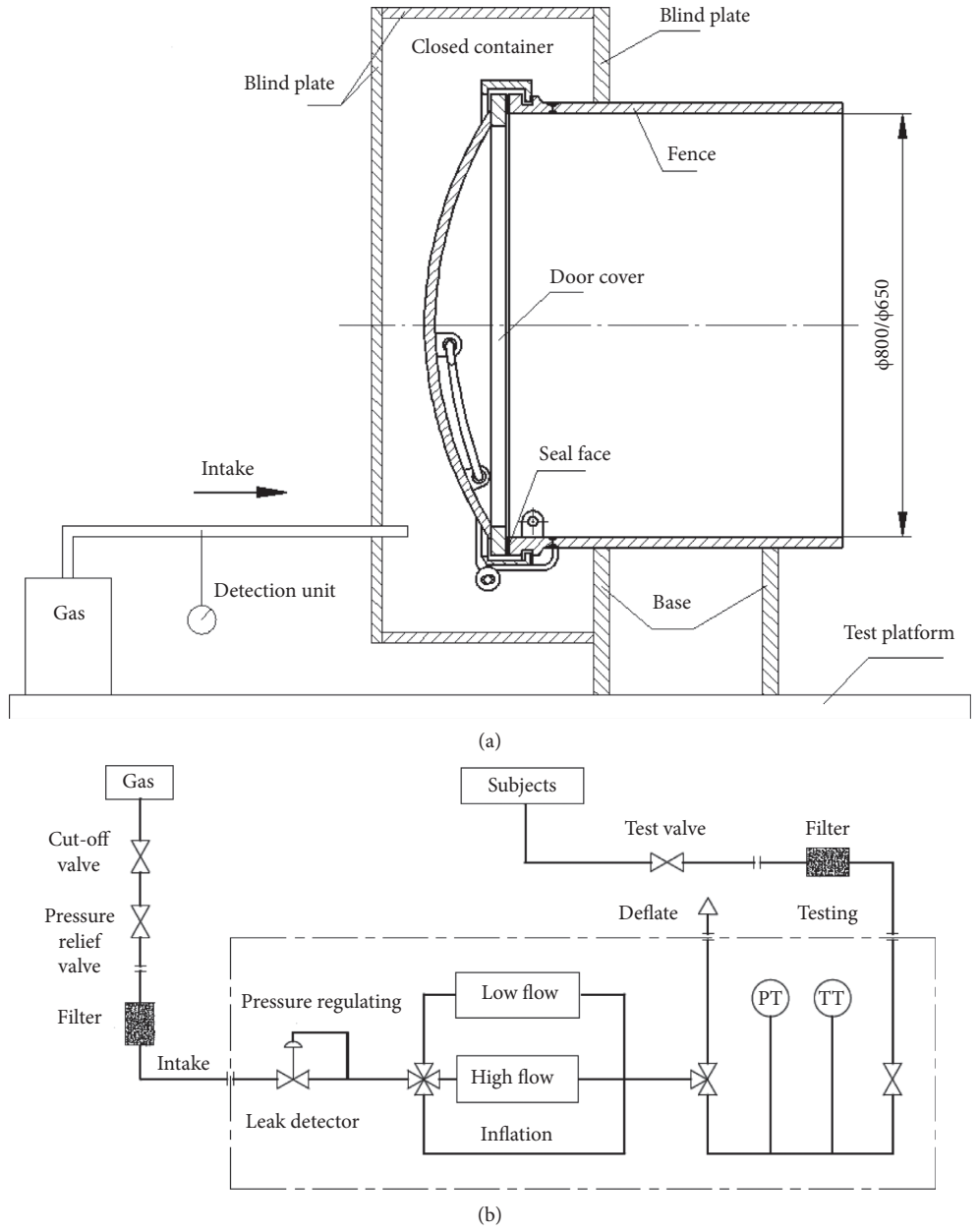

Figure 15: Dry air leakage rate test bench for pressure valve. (a) Device diagram. (b) Schematic diagram.

leakage rate of the test space. JLY-IV local leak detector developed by Beijing Metallurgical Nuclear Technology Development Co., Ltd., is adopted as the detection instrument, with flow measurement accuracy of ±3% and pressure measurement accuracy of ±0.5%. The working medium used in the test is dry air. Leakage rates under several differential pressures are measured: 0.05 MPa, 0.1 MPa, 0.15 MPa, 0.2 MPa, 0.4 MPa, and 0.6 MPa. The test principle of other penetration is similar and will not be repeated here.

Figure 16 displays the test results and theoretical calculation results of sealing rings with two hardness. In the calculation, the flange is 06Cr19Nil0 stainless steel, and surface roughness is 3.2 μm. The diameter is 800 mm. The pretightening compression ratio of the sealing ring is 12.5%. The sealing medium is dry air. The pressure of the sealing chamber gauge increases gradually from 0.05Mpa to 0.6 MPa, which simulates the process of gradual pressure rise under accident conditions. It can be seen from Figure 16, under normal pressure ($\triangle P = 0.05$ Mpa), the leakage rate of the sealing ring is only 10^{-8} kg/s, and the corresponding volume flow is less than 1 ml/min. When the pressure increases to 0.4~0.5 MPa, the leakage rate rises to the order of 10^{-6} kg/s, and the corresponding volume flow is 10~14 ml/min. These are meeting with the engineering design requirements. The data

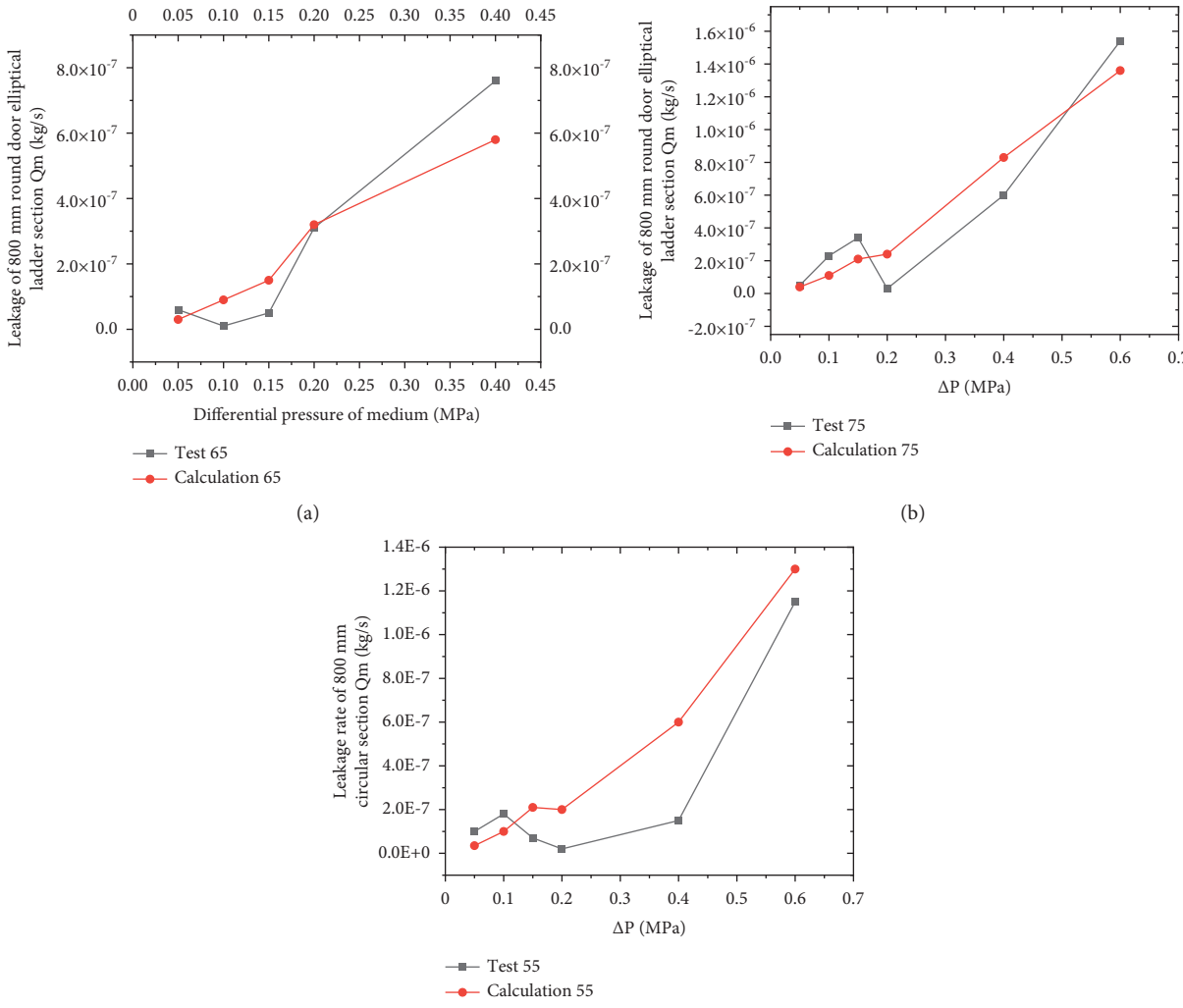

Figure 16: Comparison between measured value and theoretical predicted value of leakage rate test of pressure valve. (a) Elliptical trapezoidal section sealing ring with hardness of 65. (b) Elliptical trapezoidal section sealing ring with hardness of 77. (c) Circular section sealing ring with hardness of 55.

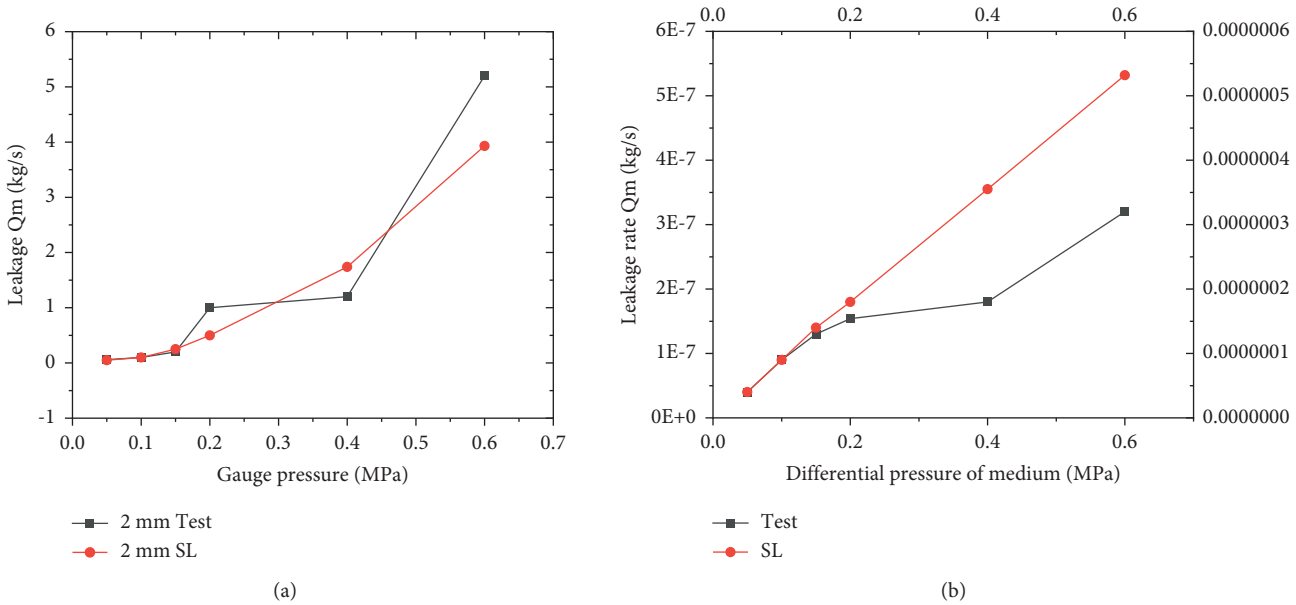

Figure 17: Continued.

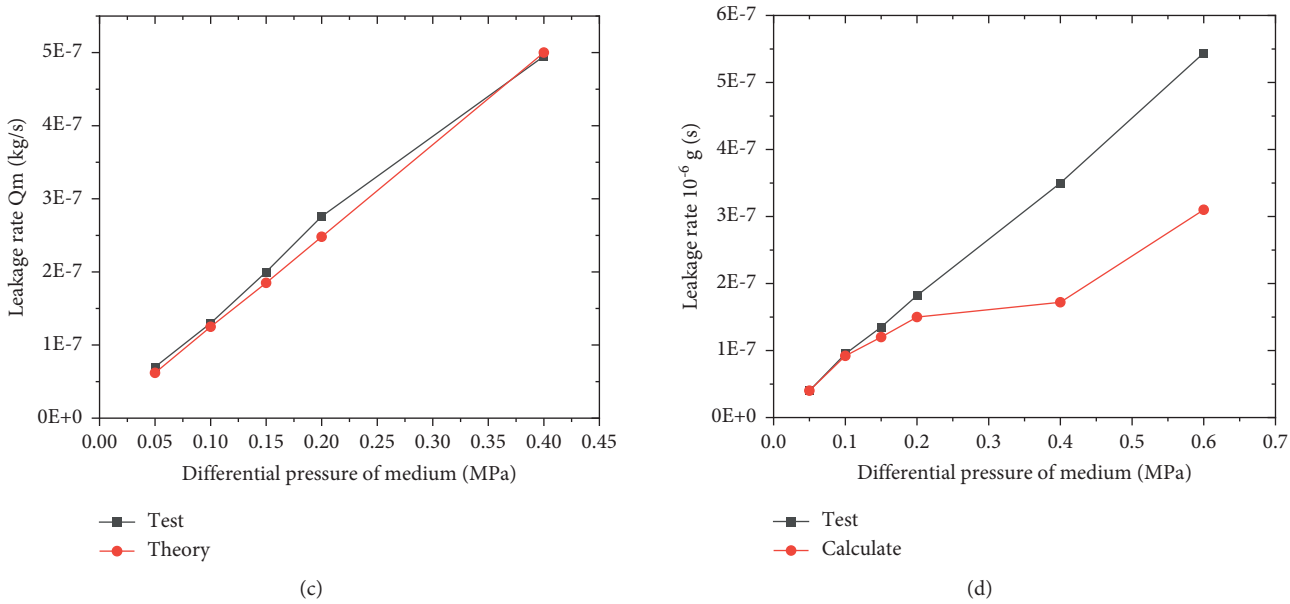

Figure 17: Comparison between theoretical and experimental values of leakage rates of several typical penetrations. (a) Lifting eye. (b) Soft cut-off valve DN65. (c) Butterfly valve. (d) Manual globe valve.

in Figure 17 show that the theoretically predicted values of the two sealing rings are in good agreement with the experimentally measured values, with the same trend and similar values, which well verifies the accuracy of the prediction method proposed in this study.

5. Conclusion

(1) In this paper, the constitutive relationship between leakage rate and microstructure parameters is established based on porous media seepage mechanics, and a new prediction model of leakage rate of sealing structure is proposed. Then, the relationship between seal specific pressure and microstructure parameters is obtained by Hertz contact mechanics model. The prediction model of penetration leakage rate established by this method is in good agreement with the experimental results, and it can better reflect the effects of rough surface morphology, material mechanical properties, sealing load, high temperature, and high pressure on the leakage rate.

(2) In the calculation, the roughness of the flange is Ra3.2, and the minimum leakage rate can be $4.9E^{-3}\,m^3$/day. When other conditions remain unchanged, the leakage rate will decrease significantly with the decrease of roughness. According to the analysis of leakage rate mechanism model, the main factors affecting the leakage rate of pressure cover include medium pressure, bolt preload, flange roughness, and so on. Within the material strength limit, try to select larger preload and lower roughness.

(3) The sealing principle of penetration can be classified as contact static seal, where interface leakage is the main leakage path of this kind of sealing structure under normal working condition. The main factors affecting the leakage rate of various penetration parts can be divided into several categories: the first is the micromorphology characterization of the contact surface of the sealing pair, that is, the composite surface roughness. The increase of roughness often leads to the magnitude change of leakage rate. The second type is the mechanical properties of sealing pair materials, especially the mechanical deformation properties of seals. When the working conditions are bad, its aging characteristics also need to be considered. The third type is the macrostructure of the sealing pair, which is often the key to the leakage rate control. The contact stresses distribution of the sealing pair produced by different structures will be quite different.

(4) It should be pointed out that there are some uncertain factors in the model calculation: ① preload; ② composite roughness of sealing pair; ③ effects of high temperature, high pressure, and high humidity on mechanical properties of rubber seals. Each of these factors will have a great impact on the leakage rate. Therefore, the theoretical research of leakage rate must be based on certain measurement results and experimental data, and then, more detailed prediction model research is performed on various penetrations.

6. Future Directions

The current research still has certain limitations, and the following aspects need to be further strengthened and improved.

(1) The numerical simulation calculation in this paper is carried out based on making assumptions and simplifies the sealing structure. In order to make the simulation results more accurate, it is necessary to establish a model more in line with the actual situation.

(2) Limited by the experimental conditions, this paper selects several typical penetrators for experiments, and more penetration experiments can be added to improve the prediction model in the future.

(3) In the future, we will further study the influencing factors affecting the leakage rate, further improve the accuracy and scope of application of this prediction model, refer to the research results of other scholars, and provide a theoretical basis for the development and design of penetration seal structure.

Data Availability

The data used to support the findings of this study are included within the article.

Conflicts of Interest

The authors have no conflicts of interest to declare that are relevant to the content of this article.

References

[1] Q. K. Chen, "Research on strain and sealing performance of mechanical penetration under limit load," *CHINA MEASUREMENT & TEST*, vol. 46, no. 1, pp. 160–168, 2020.

[2] T. Kincaid, R. Romocki, B. A. Meyer, G. Annandale, H. Falvey, and W. Hultman, "Evaluating erodibility, mitigating leakage, and addressing potential failure modes at a concrete arch dam through groundwater modeling," in *Proceedings of the Association of State Dam Safety Officials*, Seattle, DC, USA, September 2018.

[3] X. M. Huang, "Study on leak mechanism and leakage rate prediction model of reactor containment sealing structure," *Nuclear Power Engineering*, vol. 37, no. 3, pp. 116–121, 2016.

[4] W. Q. Zhou and X. P. Qiu, "The principle and data analyse of online monitoring system of containment leak rate," *Nuclear Power Engineering*, vol. 18, no. 2, pp. 153–157, 1997.

[5] M. Nakano and H. Sasaki, "Radiation resistance of rubber compounds for gaskets," in *Proceedings of the 2012 Twentyth International Conference on Nuclear Engineering*, Article ID 54985, California, CA, USA, August 2012.

[6] C. W. Zhang, Y. D. Yang, and Y. Qiao, "Principle and data analysis of on-line monitoring system for containment leakage rate," *Nuclear Safety*, vol. 13, no. 2, pp. 1672–5360, 2014.

[7] Q. K. Chen, "Research on strain and sealing performance of mechanical penetration under limit load," *China Measurement & Test*, vol. 46, no. 1, pp. 1674–5124, 2020.

[8] L. Tong, X. Zhou, and X. Cao, "Ultimate pressure bearing capacity analysis for the prestressed concrete containment," *Annals of Nuclear Energy*, vol. 121, pp. 582–593, 2018.

[9] F. Lin and H. Tang, "Nuclear containment structure subjected to commercial aircraft crash and subsequent vibrations and fire," *Nuclear Engineering and Design*, vol. 322, pp. 68–80, 2017.

[10] I. Tavakkoli, M. R. Kianoush, H. Abrishami, and X. Han, "Finite element modelling of a nuclear containment structure subjected to high internal pressure," *International Journal of Pressure Vessels and Piping*, vol. 153, pp. 59–69, 2017.

[11] S.-J. Jeon and B.-M. Jin, "Improvement of impact-resistance of a nuclear containment building using fiber reinforced concrete," *Nuclear Engineering and Design*, vol. 304, pp. 139–150, 2016.

[12] M. H. Shackelford, T. R. Bump, and R. W. Seidensticker, "Characterization of Nuclear Reactor Containment Penetrations Final Report," NUREG/CR- SAND-7139; ANL-87. ON: TI85010463, National Technical Information Service (NTIS), Springfield, VA, USA, 1985.

[13] M. Nakano, H. Sasaki, and K. Hanasima, "The prediction of long-term and emergency sealability of silicone and EPDM gaskets," in *Proceedings of the Eighteenth International Conference on Nuclear Engineering, ICONE18-30169*, Xi'an, China, May 2010.

[14] L. Marchand, M. Derenne, and V. Masi, "Predicting gasket leak rates using a laminar- molecular flow model," in *Proceedings of the ASME Pressure Vessels and Piping Conference*, pp. 87–96, Denver, CO, USA, July 2005.

[15] B. Gu, Y. Chen, and D. Zhu, "Prediction of leakage rates through sealing connections with nonmetallic gaskets," *Chinese Journal of Chemical Engineering*, vol. 15, no. 6, pp. 837–841, 2007.

[16] L. Grine and A.-H. Bouzid, "Analytical and experimental studies of liquid and gas leaks through micro and nano-porous gaskets," *Materials Sciences and Applications*, vol. 4, no. 8, pp. 32–42, 2013.

[17] P. Jolly and L. Marchand, "Leakage predictions for static gasket based on the porous media theory," *Journal of Pressure Vessel Technology*, vol. 131, no. 2, Article ID 21203, 2009.

[18] A. Abouel-Kasem, "Numerical analysis of leakage rate for the selection of elastomeric sealing materials," *Sealing Technology*, vol. 2006, no. 11, pp. 7–11, 2006.

[19] E. Roos, H. Kockelmann, and R. Hahn, "Gasket characteristics for the design of bolted flange connections of metal-to-metal contact type," *International Journal of Pressure Vessels and Piping*, vol. 79, no. 1, pp. 45–52, 2002.

[20] H. A. Saeed, S. Izumi, S. Sakai, S. Haruyama, M. Nagawa, and H. Noda, "Development of new metallic gasket and its optimum design for leakage performance," *Journal of Solid Mechanics and Materials Engineering*, vol. 2, no. 1, pp. 105–114, 2008.

[21] F. Bottiglione, G. Carbone, L. Mangialardi, and G. Mantriota, "Leakage mechanism in flat seals," *Journal of Applied Physics*, vol. 106, no. 10, pp. 1–7, 2009.

[22] Q. Zheng, J. Xu, B. Yang, and B. Yu, "A fractal model for gaseous leak rates through contact surfaces under non-isothermal condition," *Applied Thermal Engineering*, vol. 52, no. 1, pp. 54–61, 2013.